Surgery Open Science 24 (2025) 66–69

Contents lists available at ScienceDirect

Surgery Open Science

journal homepage: www.journals.elsevier.com/surgery-open-science

Research Paper

Exploring the dynamics of postoperative steatosis in the regenerating liver: An animal study

Andrea Lund [a,b,*,1], Katrine Holm Andersen [a,b,1], Kasper Jarlhelt Andersen [a], Jakob Kirkegård [a,b], Jens Randel Nyengaard [c,d], Frank Viborg Mortensen [a,b]

[a] Department of Surgery, Section for HPB Surgery, Aarhus University Hospital, Aarhus, Denmark
[b] Department of Clinical Medicine, Aarhus University, Aarhus, Denmark
[c] Core Center for Molecular Morphology, Section for Stereology and Microscopy, Aarhus University, Denmark
[d] Department of Pathology, Aarhus University Hospital, Denmark

ARTICLE INFO

Keywords:
Liver regeneration
Partial hepatectomy
Hepatic steatosis
Rat
Lipid accumulation

ABSTRACT

Introduction: The rat model of 70 % partial hepatectomy (PH) is commonly used to investigate liver regeneration processes. The aim of this study was to explore the dynamics of hepatic lipid accumulation and its correlation with the proliferation response during the entire regeneration phase after 70 % PH in rats.
Methods: Sixty-four rats underwent 70 % PH and were randomly divided into eight groups for evaluation on post-operative day (POD) 1 to 8. Hepatocyte volume, relative lipid content, and lipid volume per hepatocyte were assessed by stereological analysis.
Results: Lipid volume per hepatocyte reached its peak on POD 1 and POD 2, with mean values of 2895 μm^3 (95 % CI: 1756–4034 μm^3) and 3090 μm^3 (95 % CI: 2277–3903 μm^3), respectively. A marked decline was observed by POD 4, with a mean of 1323 μm^3 (95 % CI: 985–1741 μm^3), which continued through POD 5, reaching 619 μm^3 (95 % CI: 136–1102 μm^3). From POD 5 onwards, lipid volume remained consistently low, with no significant differences detected between POD 5 and POD 8.
Conclusion: Lipid accumulation and proliferation peak and decline concurrently, suggesting a strong correlation.

Introduction

Partial hepatectomy (PH) is the gold standard for treating both primary and secondary liver malignancies. In healthy livers, up to 70 % of the parenchyma can be resected without compromising the liver's ability to maintain body homeostasis [1]. This is facilitated by its unique regenerative capacity and substantial metabolic reserves. To improve outcomes following PH, a deeper understanding of the mechanisms underlying liver regeneration is important. Such knowledge could lead to the development of novel treatment strategies aimed at optimizing conditions for liver regeneration, potentially increasing the number of patients eligible for surgical treatment.

It has been suggested that transient post-PH steatosis may play a crucial role in facilitating successful liver regeneration, potentially by providing lipids as essential building blocks, energy sources, and signalling molecules required for the initiation of cell proliferation [2–7]. However, the precise relationship between lipid accumulation and hepatocyte proliferation during liver regeneration remains insufficiently elucidated. Moreover, the dynamics of lipid accumulation and correlation to proliferation throughout the entire liver regeneration process, from PH to complete liver volume restoration, remains inadequately investigated. A comprehensive understanding of these dynamic changes is essential, as distinct phases of regeneration may offer opportunities for targeted interventions aimed at optimizing liver recovery and improving therapeutic strategies.

We have previously investigated the proliferation response following 70 % PH in rodents [8]. Since the rat liver regenerates within 7–8 days after 70 % PH[2], our experiment was designed to cover this timeframe. In

Abbreviations: PH, partial hepatectomy; POD, post-operative day; CI, confidence interval.

* Corresponding author at: Department of Surgery, Section for HPB Surgery, Aarhus University Hospital, Palle Juul-Jensens Boulevard 99, DK-8200 Aarhus N, Denmark.
E-mail address: Andrealund@clin.au.dk (A. Lund).

[1] Shared first authorship.

https://doi.org/10.1016/j.sopen.2025.02.005
Received 8 February 2025; Accepted 18 February 2025
Available online 21 February 2025

this study, we aimed to examine the progression of hepatic steatosis during liver regeneration, enabling a direct comparison between hepatocyte proliferation and lipid accumulation. Furthermore, we sought to identify specific time points within this surgical model that could serve as potential targets for future research focused on evaluating metabolic interventions to enhance liver regeneration.

Methods

Ethical approval

The experiment was performed under the approval of the Danish Animal Research Committee, Copenhagen, Denmark, under the license number 2009/561–1752, and in accordance with the "Guide for the Care and Use of Laboratory Animals" published by the National Institutes of Health, USA. The experiment is reported according to the ARRIVE guidelines [9]. All animals were housed in standard cages at a temperature of 23 °C, with unlimited supply of food and water, and an artificial 12-h light-dark cycle.

Experimental design

Sixty-four rats were subjected to 70 % PH. The surgical and anaesthetic procedures have previously been described in detail [8]. In brief, the 70 % PH was performed by resection of the left lateral lobe and median lobe of the liver, leaving the right superior lobe, right inferior lobe, anterior caudate lobe, and posterior caudate lobe intact.

Following surgery, animals were block-randomized for evaluation on post-operative day (POD) 1 to 8. Five animals were euthanized prior to evaluation; one due to suture gnawing, one to ileus, and three to undetermined causes. To maintain a total of eight animals per group, five additional animals were subjected to PH. At euthanisation, the liver remnant was removed for further analysis.

In our initial investigation, we compared animals regarding proliferating hepatocytes by quantifying Ki-67 expression on each POD [8]. In the current study, liver tissue from the same cohort of animals was analysed to determine lipid accumulation in the regenerating livers. This approach enabled a comparative analysis between Ki-67 levels and lipid accumulation.

Stereology

The anterior caudate lobe was prepared for stereological analysis following a previously published in-house protocol [8]. Stereological analyses were conducted using an Olympus BX50 microscope with a motorized stage (Märzhäuser Wetzlar MFD, Wetzlar, Germany) and a digital camara (Olympus DP73, Olympus, Tokyo, Japan) connected to a computer running newCAST version 2020.01.4.8088 software (Visiopharm, Hørsholm, Denmark).

All analyses were performed by an investigator who was blinded to the POD group from which the tissues samples were derived. For each animal, two 2 μm thick sections were analysed, with an average of 20 systematically, uniformly, and randomly selected fields of view per section. To estimate the relative lipid content per hepatocyte, a 6 × 4 point grid with green and blue test points was used (Fig. 1A). Each test point, whether blue and green, that intersected with a lipid droplet was counted as lipid, while each blue test intersecting with a hepatocyte was counted as a hepatocyte. Lipid droplets were defined as clear vacuoles [10], validated by electron microscopy (Fig. 1B and C).

To estimate the relative lipid content per hepatocyte, the following formula was used:

$$V_v(\text{lipid per hepatocyte}) = \frac{\sum P(\text{lipid})}{\sum P(\text{hepatocyte})}$$

where $\sum$P(lipid) represents the sum of test point intersecting with a lipid droplet, and $\sum$P(hepatocyte) represents the sum of the blue test points intersecting with a hepatocyte.

The relative lipid content within hepatocytes was estimated using a point grid marked with green and blue test points (Fig. 1A). Each test point intersecting with a lipid droplet was counted as lipid, while only the blue test points intersecting with a hepatocyte were counted as such.

To estimate the volume of lipid per hepatocyte, the individual hepatocyte volume was first determined using the 3D isotropic nucleator

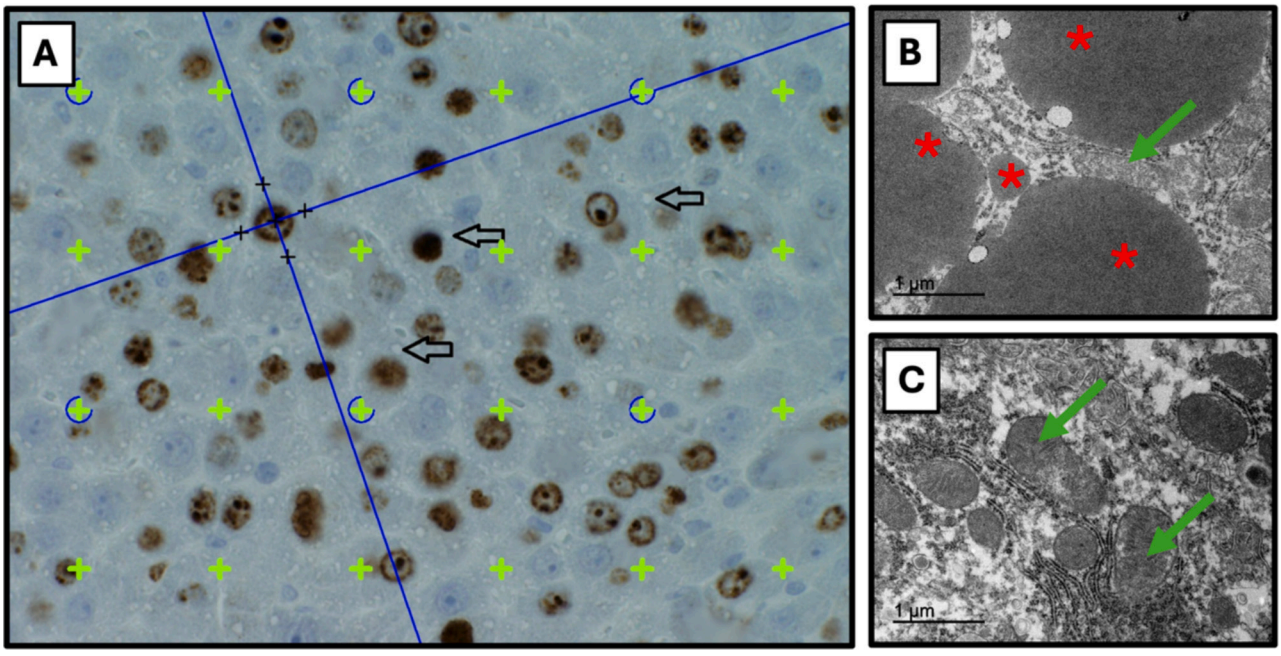

Fig. 1. Lipid accumulation visualized by light microscopy and transmission electron microscopy. (A) Liver section from a POD 1 animal. Ki-67 and hematoxylin staining. Lipid droplets are represented by clear vacuoles (black arrows). (B) Electron microscopy image of a hepatocyte from a POD 1 animal with huge lipid droplets (*) surrounded by mitochondria (green arrow). (C) Electron microscopy image of a hepatocyte from a POD 8 animal with mitochondria (green arrows) but no lipid droplets. (For interpretation of the references to colour in this figure legend, the reader is referred to the web version of this article.)

(Fig. 1A) [11,12]. The nucleator probe was applied to two randomly sampled hepatocytes per fields of view, using 40 fields of view per animal. Two systematic and random test lines intersecting the hepatocyte nucleus were generated. The points of interception between the test lines and the cell boundary were marked. The software subsequently calculates the cell volume based on the distances along these test lines.

The following formula was used to calculate the volume of lipid per hepatocyte:

$$V(\text{lipid in hepatocyte}) = V_v(\text{lipid per hepatocyte}) \cdot V(\text{hepatocyte})$$

where V(hepatocyte) represents the mean hepatocyte volume.

Transmission electron microscopy

Cubes from the fixed posterior lobe (2 mm^3) were processed and embedded in resin using the Standard TAAB 812 Resin Kit (TAAB Laboratory Equipment Ltd., Berks, UK), following standard protocols for transmission electron microscopy. Ultrathin sections were prepared with an ultramicrotome (Leica Microsystems, Wetzlar, Germany), and transmission electron microscopy images were captured with a JEM-1010 electron microscope (JEOL Ltd., Akishima, Tokyo, Japan) equipped with an Orius SC1000 CCD digital camera (Gatan, Inc., Pleasanton, CA, USA).

Statistical analysis

The data was tested for normality using histograms and QQ-plots. If normality was violated, the data was log-transformed prior to analysis and then back transformed. Comparisons across all groups were conducted using the analysis of variance, while unpaired *t*-tests were used for direct comparisons between two groups. Parametric data are presented as mean values, while non-parametric data are expressed as medians. All data are presented with 95 % confidence intervals (CIs). Statistical significance was determined by *p*-values with a significance threshold at p-values <5 % and by overlapping CIs. Statistical analysis was performed using Stata 17.0 (StataCorp, College Station, TX, U.S).

Results

The median relative lipid content per hepatocyte and mean hepatocyte volume across all POD groups are summarized in Table 1.

The lipid volume per hepatocyte peaked on POD 1 and POD 2 with means of 2895 μm^3 (95 % CI: 1756 μm^3–4034 μm^3) and 3090 μm^3 (95 % CI: 2277 μm^3–3903 μm^3), respectively (Fig. 2). A non-significant reduction was observed on POD 3, with a mean of 2288 μm^3 (95 % CI: 1980 μm^3–2595 μm^3). By POD 4, the decline became significant compared to POD 2 and POD 3, reaching a mean of 1323 μm^3 (95 % CI: 985 μm^3–1741 μm^3). This downward trend persisted through to POD 5, with a mean of 619 μm^3 (95 % CI: 136 μm^3–1102 μm^3). From POD 5, the lipid volume per hepatocyte remained low, with no significant differences observed between the groups.

Table 1
Hepatocyte morphology. Median relative hepatocyte lipid content and mean hepatocyte volume, each presented with their respective 95 % CIs.

	Relative hepatocyte lipid content (%)	Hepatocyte volume (μm^3)
POD 1	46 (32–66)	6663 (5607–7719)
POD 2	49 (37–64)	6575 (5902–7247)
POD 3	34 (29–40)	6910 (6452–7369)
POD 4	23 (16–31)	6422 (5742–7102)
POD 5	6 (2–14)	5488 (4693–6283)
POD 6	6 (3–10)	5482 (4705–6260)
POD 7	7 (4–10)	5356 (4564–6149)
POD 8	10 (5–17)	5517 (4421–6613)

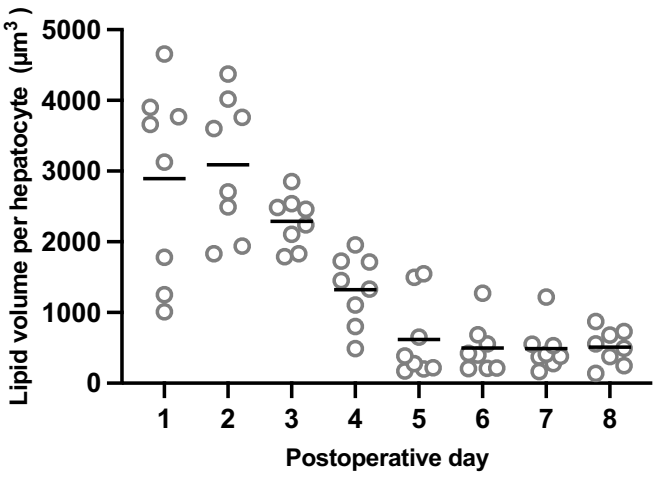

Fig. 2. Lipid volume per hepatocyte. Each dot represents one animal. The median in each group is illustrated by a black line.

Discussion

In this study, stereological quantifications were employed to examine the dynamics of lipid accumulation throughout the entire liver regeneration phase following 70 % PH in rats. Additionally, we explored the correlation between hepatic lipid accumulation and hepatocyte proliferation during liver regeneration. We observed that lipid accumulation peaked at POD 1 and POD 2, followed by a significant decrease by POD 4. This decline persisted through POD 5, after which lipid levels remained low for the remainder of the experiment.

In our previous experiment, we found that hepatocyte proliferation peaked between POD 1–3, declined by POD 4, and returned to baseline levels, with near no proliferation, by POD 5 [8]. Our current findings on lipid accumulation dynamics align closely with our previous observations on hepatocyte proliferation. The parallel pattern suggests a potential relationship between lipid accumulation and hepatocyte proliferation during the entire liver regeneration period, where the peak in lipid accumulation coincide with the peak in hepatocyte proliferation, and the subsequent decline in lipid accumulation mirrors the reduction in proliferative activity. These findings support the idea that lipid availability could be closely linked to the regenerative process of the liver, as suggested by other [3–5,7,13].

Nevertheless, there are some discrepancies in the evidence, as some studies report a correlation between the extent of lipid accumulation and hepatocyte proliferation, while others do not observe the same relationship [14,15]. These discrepancies, however, might in part be explained by studies investigating preoperative steatosis rather than postoperative steatosis, which are different conditions.

Research in rodents have indicated that enhancing the lipid metabolism or lipid uptake in hepatocytes following PH improves liver regeneration [16]. Thus, this approach might be a promising treatment strategy in the future to reduce the risk of post-hepatectomy liver failure or to make more patients eligible for surgery.

A key strength of our study lies in the application of stereological methods, which offer precise, randomized, and unbiased estimates of lipid volume per hepatocyte, effectively avoiding the risk of the reference trap [11,12]. Notably, while hepatocyte volume was measured to ensure the most accurate assessment of relative lipid content per hepatocyte, it was not employed as a surrogate for hepatocyte proliferation, which was directly evaluated using Ki-67 antibody in our prior study [8]. Hepatocyte volume was considered due to the potential size fluctuations that hepatocytes undergo during liver regeneration. By accounting for this variability, we ensured a more accurate quantification of lipid content per hepatocyte. Furthermore, the randomization of rats into the respective POD groups was implemented to minimize potential

bias arising from litter-related variability.

One potential limitation of our study is the lack of direct lipid staining, such as the Oil Red O, which might have led to an underestimation of lipid droplets. Nevertheless, our hematoxylin-based lipid assessments were validated using electron microscopy (Fig. 1B), and the approach was deemed sufficient for our study. Another challenge was the absence of specific staining techniques, such as the β-catenin staining, which marks the cell membranes and aids in precisely visualizing cell boundaries for accurate hepatocyte volume measurements. Despite this, Fig. 1A illustrated that cell boundaries were sufficiently discernible, rendering our approach suitable for the analyses conducted.

In conclusion, our findings demonstrate that hepatocyte lipid accumulation and proliferation peak simultaneously, followed by a concurrent decline, highlighting a strong correlation between these processes.

Our study provides novel insights into the dynamics of lipid accumulation throughout the entire liver regeneration process, offering valuable knowledge for future research on liver regeneration in general and metabolic alterations following PH in particular. Further studies are needed to clarify the specific roles of lipids in liver regeneration and to explore potential therapeutic applications, such as promoting liver regeneration through lipid metabolism regulation. This study also highlights key timepoints within this well-established surgical rat model that could be utilized for such investigations.

CRediT authorship contribution statement

Andrea Lund: Conceptualization, Data curation, Formal analysis, Funding acquisition, Investigation, Methodology, Project administration, Supervision, Visualization, Writing – original draft, Writing – review & editing. **Katrine Holm Andersen:** Data curation, Investigation, Writing – original draft, Writing – review & editing. **Kasper Jarlhelt Andersen:** Conceptualization, Data curation, Investigation, Project administration, Writing – review & editing. **Jakob Kirkegård:** Formal analysis, Supervision, Writing – review & editing. **Jens Randel Nyengaard:** Conceptualization, Formal analysis, Methodology, Supervision, Writing – review & editing. **Frank Viborg Mortensen:** Conceptualization, Formal analysis, Funding acquisition, Methodology, Project administration, Supervision, Writing – review & editing.

Author contributions

Lund A, Andersen KJ, and Mortensen FV performed the study conception and design. Data collection was performed by Andersen KJ, Andersen KH, and Lund A. Analyses and interpretation of data were performed by Lund A, Andersen KH, Kirkegård J, Nyengaard JR, and Mortensen FV. The manuscript was drafted by Lund A and Andersen KH. Critical revision and approval of the final paper were performed by Lund A, Andersen KH, Kirkegård J, Andersen KJ, Nyengaard JR, and Mortensen FV.

Ethics approval

This study is approved by the Danish National Committee for the Protection of Animals used for Scientific Purposes, Copenhagen, Denmark, under the license number 2009/561–1752.

Financial disclosure

The funding sources had no role in the intervention, data interpretation, or drafting of the manuscript. All funding was provided by Andrea Lund.

Funding

This work was supported by Dagmar Marshalls Foundation and A.P. Møller Foundation.

Declaration of competing interest

The authors declare that they have no known competing financial interests or personal relationships that could have appeared to influence the work reported in this manuscript.

Acknowledgements

The authors thank Dagmar Marshalls Foundation and A.P. Møller Foundation for funding this research. We also thank Trine Werenberg Mikkelsen for her excellent technical assistance.

References

[1] Guglielmi A, Ruzzenente A, Conci S, Valdegamberi A, Iacono C. How much remnant is enough in liver resection? Dig Surg 2012;29(1):6–17. https://doi.org/10.1159/000335713.
[2] Michalopoulos GK, Bhushan B. Liver regeneration: biological and pathological mechanisms and implications. Nat Rev Gastroenterol Hepatol 2021;18(1):40–55. https://doi.org/10.1038/s41575-020-0342-4.
[3] Lund A, Thomsen MT, Kirkegård J, Knudsen AR, Andersen KJ, Meier M, et al. Role of steatosis in preventing post-hepatectomy liver failure after major resection: findings from an animal study. J Clin Exp Hepatol 2025;15(2):102453. https://doi.org/10.1016/j.jceh.2024.102453.
[4] Solhi R, Lotfinia M, Gramignoli R, Najimi M, Vosough M. Metabolic hallmarks of liver regeneration. Trends Endocrinol Metab 2021;32(9):731–45. https://doi.org/10.1016/j.tem.2021.06.002.
[5] Zabielski P, Baranowski M, Zendzian-Piotrowska M, Blachnio A, Gorski J. Partial hepatectomy activates production of the pro-mitotic intermediates of the sphingomyelin signal transduction pathway in the rat liver. Prostaglandins Other Lipid Mediat 2007;83(4):277–84. https://doi.org/10.1016/j.prostaglandins.2007.02.001.
[6] Kmieć Z. Cooperation of liver cells in health and disease. Adv Anat Embryol Cell Biol 2001;**161**(Iii-xiii):1–151. https://doi.org/10.1007/978-3-642-56553-3.
[7] Fernández MA, Albor C, Ingelmo-Torres M, Nixon SJ, Ferguson C, Kurzchalia T, et al. Caveolin-1 is essential for liver regeneration. Science 2006;313(5793):1628–32. https://doi.org/10.1126/science.1130773.
[8] Andersen KJ, Knudsen AR, Kannerup AS, Sasanuma H, Nyengaard JR, Hamilton-Dutoit S, et al. The natural history of liver regeneration in rats: description of an animal model for liver regeneration studies. Int J Surg 2013;11(9):903–8. https://doi.org/10.1016/j.ijsu.2013.07.009.
[9] Percie du Sert N, Hurst V, Ahluwalia A, Alam S, Avey MT, Baker M, et al. The ARRIVE guidelines 2.0: updated guidelines for reporting animal research. PLoS Biol 2020;18(7):e3000410. https://doi.org/10.1371/journal.pbio.3000410.
[10] Chan JK. The wonderful colors of the hematoxylin-eosin stain in diagnostic surgical pathology. Int J Surg Pathol 2014;22(1):12–32. https://doi.org/10.1177/1066896913517939.
[11] Møller A, Strange P, Gundersen HJ. Efficient estimation of cell volume and number using the nucleator and the disector. J Microsc 1990;159(Pt 1):61–71. https://doi.org/10.1111/j.1365-2818.1990.tb03019.x.
[12] Gundersen HJ. The nucleator. J Microsc 1988;151(Pt 1):3–21. https://doi.org/10.1111/j.1365-2818.1988.tb04609.x.
[13] Farrell GC. Probing Prometheus: fat fueling the fire? Hepatology 2004;40(6):1252–5. https://doi.org/10.1002/hep.20522.
[14] Hamano M, Ezaki H, Kiso S, Furuta K, Egawa M, Kizu T, et al. Lipid overloading during liver regeneration causes delayed hepatocyte DNA replication by increasing ER stress in mice with simple hepatic steatosis. J Gastroenterol 2014;49(2):305–16. https://doi.org/10.1007/s00535-013-0780-7.
[15] DeAngelis RA, Markiewski MM, Taub R, Lambris JD. A high-fat diet impairs liver regeneration in C57BL/6 mice through overexpression of the NF-kappaB inhibitor, IkappaBalpha Hepatology 2005;42(5):1148–57. https://doi.org/10.1002/hep.20879.
[16] Bláha V, Simek J, Zadák Z. Liver regeneration in partially hepatectomized rats infused with carnitine and lipids. Exp Toxicol Pathol 1992;44(3):165–8. https://doi.org/10.1016/s0940-2993(11)80155-7.